SF_6/O_2 Plasma Nanotexturing of Silicon:
Decoupling How Ion Flux and Ion Energy Matter

G. Fischer[1,2], E. Drahi[3], S. A. Filonovich[3], E. V. Johnson[1,2]

[1]Institut Photovoltaïque d'Ile-de-France (IPVF), 30 RD 128, 91120 Palaiseau, France
[2]LPICM, CNRS, Ecole polytechnique, Université Paris-Saclay, 91128 Palaiseau, France
[3]Total SA Renewables, 24 cours Michelet, La Défense 10, 92069 Paris la Défense Cedex, France

1. Introduction

Crystalline silicon (c-Si) solar cell performance can be improved by reducing front surface reflectance. A drastic decrease may be obtained by texturing the silicon surface at the nanoscale ("nanotexturing"), leading to a graded refractive index between air and c-Si. This so-called "black silicon" has been successfully applied to photovoltaic devices [1,2]. SF_6/O_2 plasma etching of silicon in a capacitively coupled radiofrequency (CCP-RF) discharge is known to induce spontaneous nanotexturing [3]. This phenomenon – typically resulting in the formation of conical nanostructures (NS) with typical sizes ranging from 30 to 500 nm – occurs through in-situ formation of non-volatile inhibitors on the surface. The latter compete with simultaneous physical and chemical etching [4], and all these mechanisms may be influenced by ions impinging the surface.

In the present study, the Ion Energy Distribution (IED) at the substrate electrode is tuned using Tailored Voltage Waveforms (TVWs) excitation in a reactive ion etching (RIE) system, aiming at the identification of the influence of ion bombardment on the dry nanotexturing process. TVWs are obtained by adding harmonic frequencies with controlled amplitudes and phase-shifts to the basis driving signal (at 13.56 MHz) [5]. This technique may give rise to amplitude and slope asymmetries in electronegative plasmas [6] such as the SF_6/O_2 mixture under consideration.

2. Experimental methods

a. Process control and monitoring

The RIE system is composed of 20 cm diameter circular aluminum plates with an interelectrode distance of 3.5 cm, enclosed in a 25 cm large cylindrical chamber. The discharge is either powered by standard RF voltage or using TVWs, with waveforms at the electrode controlled using a feedback loop, similarly to the system described in [7]. Waveforms used in this study are illustrated in Figure 1.
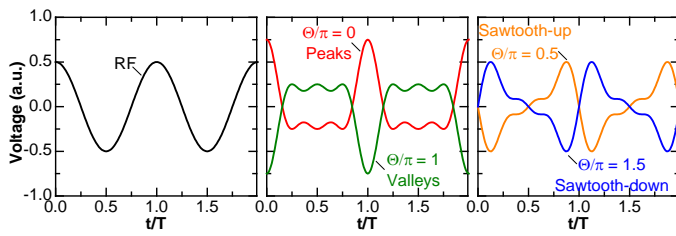
Fig. 1: Model waveforms used in the study.

The energy distribution $f(E)$ of positive ions impinging on the substrate electrode has been measured along the electrode radius using a Retarding Field Energy Analyzer (RFEA) purchased from Impedans. In particular, the total positive ion flux ϕ and the average ion bombardment energy E_{avg} are extracted.

b. Characterization of textured samples

Czochralski grown n-type c-Si substrates with (100) orientation have been textured and then characterized with the following methods: (i) Stylus profilometry is performed to assess the etch rate; (ii) Scanning Electron Microscopy (SEM) top and cross-section view images are taken to determine the characteristic NS sizes; (iii) Spectrophotometry is used to measure the total hemispherical reflectance R at normal incidence in the wavelength range [250, 1100 nm]. Quantitative comparison is given by the effective reflectance, R_{eff}, which corresponds to the average reflectance in the measured interval, weighted by the solar irradiance (ASTM AM1.5g standard).

3. Results

a. Ion flux radial non-uniformity

Spatial uniformity of the ion flux has first been assessed with the following conditions: 25 W power, at 30 mTorr with a total incoming gas flux of 105 sccm (SF_6/O_2 ratio 1.3/1), corresponding to conditions investigated in [8]. Figure 2 shows the radial profile of the ion flux and average ion bombardment energy (E_{avg}) for different driving waveforms.
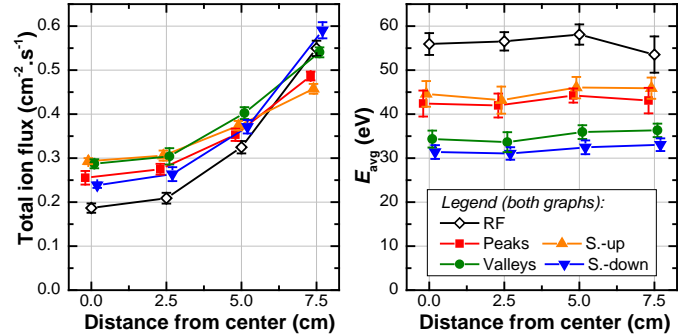
Fig. 2: Variation of the ion flux (left) and average ion bombardment energy (right) along the electrode radius with different driving voltages (25 W, 30 mTorr).

E_{avg} is constant (within the uncertainties) along the electrode radius in all conditions. The highest value is obtained for the RF case. For TVW excitation, variations of E_{avg} stem from a dominant slope asymmetry (lowest value for sawtooth-down waveforms and highest for sawtooth-up waveforms). Concerning the ion flux, an edge high profile is observed with a center to edge variation up to a factor 3 in the RF case. For the tested TVWs, the ion flux profiles remain similar to the RF case, although the center-to-edge variation is decreased (between 1.6 for sawtooth-up and 2.5 for sawtooth-down waveforms).

Although the root cause of this radial non-uniformity remains to be understood, we will take advantage of it to investigate the influence of ion flux and ion energy on the nanotexturing process.

b. Energy-dependent etching yield

Silicon samples have been processed for various durations and driving voltage waveforms while other discharge parameters (power, pressure, gas mixture) were kept constant. For each condition, four 2×2 cm^2 c-Si samples were placed along a radius of the powered electrode (same locations as the RFEA measurements presented previously).

Figure 3(a,b) shows the evolution of the etch depth d, and R_{eff} for RF, sawtooth-up and sawtooth-down waveforms at 25 W. We observe that d increases linearly with the ion fluence Φ, with a significantly lower slope in the case of sawtooth-down waveforms. As these waveforms produce a much lower E_{avg} this suggests energy-dependent etching yield. On the other hand, R_{eff} first sharply decreases for RF and sawtooth-up waveforms, before reaching a plateau. A similar behavior seems to occur with sawtooth-down waveforms excitation although at a slower pace. We therefore propose a phenomenological model based on literature [9] to define the energy weighted ion fluence Γ:

$$\Gamma = \int_{E_{th}}^{E_{max}} f(E)\left(E^{1/2} - E_{th}^{1/2}\right)dE$$

where E_{th} is an energy threshold: a value of 13 eV is found to maximize the coefficient of determination in the linear least square regression of d vs Γ. In figure 3(c,d), d and R_{eff} are shown again, this time versus Γ.
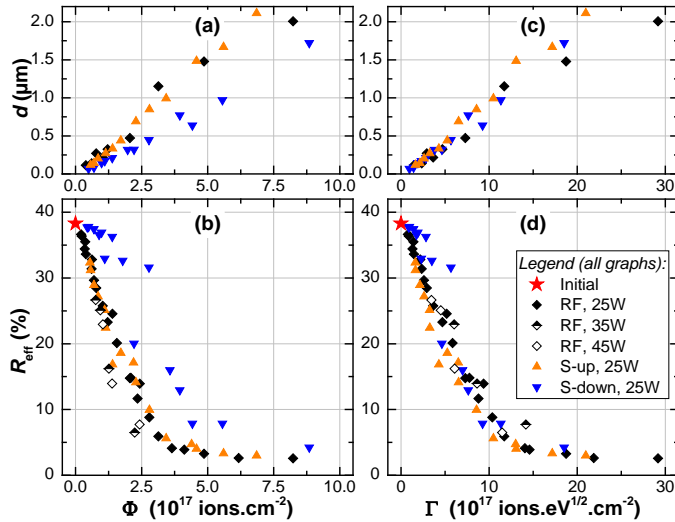
Fig. 3: (a) Etch depth and (b) effective reflectance versus ion fluence. (c,d) show the same set of data versus energy weighted ion fluence.

The proposed phenomenological model is of great interest from the point of view of process development as it directly links the final optical properties with the process conditions. However, a closer look at the nanostructures is needed to understand the evolution of R_{eff}.

c. Tuning nanostructure aspect ratio

Figure 4(a,b) shows the evolution of the nanostructures (NS) average height, h, and aspect ratio, AR, as a function of the ion fluence Φ, for samples experiencing different total ion fluxes. The linear evolution of h explains the previously mentioned decrease of reflectance: the smoother the gradient of refractive index from air to c-Si, the lower the reflectance. In contrast, the NS aspect ratio evolves differently depending on the instantaneous total ion flux. For samples exposed to the highest flux, AR rapidly increases up to values around 2, while the increase is slower for samples exposed to lower fluxes.

SEM images in Figure 4(c,d) illustrate this phenomenon: both selected samples were subjected to a similar fluence ($\Phi = 2.1\times10^{17}$ ions.cm^{-2}). NS on sample S1 are approximately 120 nm high with an aspect ratio of 1.9, while sample S2 possesses higher NS (around 160 nm) but with a lower aspect ratio of 1.3. This difference may be explained by the difference in instantaneous total ion flux ϕ (three times higher for sample S1 compared to S2). We suggest that a higher total ion flux promotes etching and prevents lateral expansion of the inhibitor layer on the flanks of the NS, leading to steeper profiles.
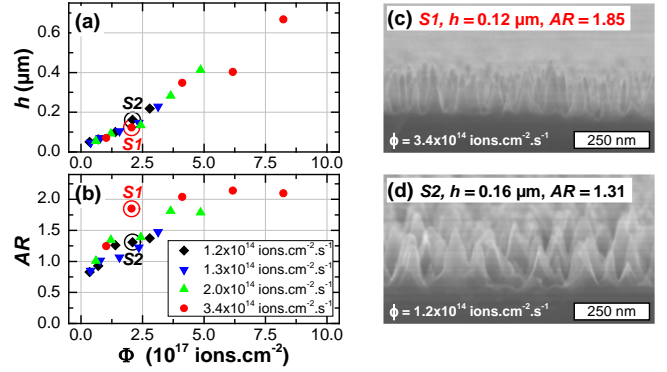
Fig. 4: (a) NS height and (b) aspect ratio versus ion fluence for different values of flux (RF excitation, 25W). (c,d) SEM images of selected samples.

4. Conclusion

Using TVWs to tune the ion energy distribution and taking advantage of the edge-high ion flux radial profile in the reactor allowed the investigation of ion flux and energy effects on nanotexturing of silicon surfaces in SF_6/O_2 plasma. Clear trends for the nanostructure formation (in terms of etch depth, NS size and shape) and the final optical properties of textured surfaces are observed using a simple phenomenological model of energy-dependent etching yield.

Increased nanostructure height reduces final reflectance, whereas increased aspect ratio will significantly enlarge the surface area and will subsequently affect surface passivation required for photovoltaic applications [10]. Design rules for the efficient implementation of this process can therefore be drawn from this study.

5. Acknowledgments

6. References

[1] M. Otto *et al.*, *Adv. Opt. Mater.* **2015**, *3*, 147.

[2] H. Savin *et al.*, *Nature Nanotech.* **2015**, *10*, 624.

[3] H. Jansen, M. de Boer, R. Legtenberg, and M. Elwenspoek, *J. Micromechanics Microengineering* **1995**, *5*, 115.

[4] M. Schnell, R. Ludemann, and S. Schaefer, *Conference records of the 28th IEEE-PVSC*, **2000**, pp. 367–370.

[5] J. Schulze, E. Schüngel, and U. Czarnetzki, *J. Phys. D: Appl. Phys.* **2009**, *42*, 092005.

[6] B. Bruneau, T. Gans, D. O'Connell, A. Greb, E. V. Johnson, and J.-P. Booth, *Phys. Rev. Lett.* **2015**, *114*.

[7] E. V. Johnson, S. Pouliquen, P.-A. Delattre, and J.-P. Booth, *Jap. J. Appl. Phys.* **2012**, *51*, 08HF01.

[8] G. Fischer, E. Drahi, M. Foldyna, T. A. Germer, and E. V. Johnson, *Opt. Express, OE* **2017**, *25*, A1057.

[9] C. Steinbrüchel, *Appl. Phys. Lett.* **1989**, *55*, 1960.

[10] G. Fischer, E. Drahi, F. Lebreton, P. Bulkin, G. Poulain, and E. V. Johnson, *Proceedings of the 33rd EU-PVSEC* **2017**, 679.